

Thermoelastic properties and crystal structure of MgSiO3 perovskite at lower mantle pressure and temperature conditions

G. Fiquet, A. Dewaele, D. Andrault, M. Kunz, T. Le Bihan

▶ **To cite this version:**

G. Fiquet, A. Dewaele, D. Andrault, M. Kunz, T. Le Bihan. Thermoelastic properties and crystal structure of MgSiO3 perovskite at lower mantle pressure and temperature conditions. Geophysical Research Letters, 2000, 27, pp.21-24. 10.1029/1999GL008397 . insu-03596953

HAL Id: insu-03596953
https://insu.hal.science/insu-03596953

Submitted on 4 Mar 2022

HAL is a multi-disciplinary open access archive for the deposit and dissemination of scientific research documents, whether they are published or not. The documents may come from teaching and research institutions in France or abroad, or from public or private research centers.

L'archive ouverte pluridisciplinaire **HAL**, est destinée au dépôt et à la diffusion de documents scientifiques de niveau recherche, publiés ou non, émanant des établissements d'enseignement et de recherche français ou étrangers, des laboratoires publics ou privés.

Copyright

GEOPHYSICAL RESEARCH LETTERS, VOL. 27, NO. 1, PAGES 21-24, JANUARY 1, 2000

Thermoelastic properties and crystal structure of $MgSiO_3$ perovskite at lower mantle pressure and temperature conditions

G. Fiquet,[1,2] A. Dewaele,[1] D. Andrault,[3] M. Kunz [4] and T. Le Bihan [5]

Abstract. A new synchrotron X-ray diffraction study of $MgSiO_3$ perovskite at high-pressure and high-temperature has been carried out in a laser-heated diamond-anvil cell to 94 GPa and temperatures above 2500 K. $MgSiO_3$ perovskite is shown to be stable in this P-T range and adopts an orthorhombic structure (space group *Pbnm*), thus ruling out any phase transition or decomposition to an assemblage of denser oxides. Structural refinements show an increase of the orthorhombic distortion with increasing pressure, counterbalanced by a decrease of this distortion at high temperature, as evidenced by the Si-O-Si angle evolution. In addition, thermoelastic parameters identified from this new pressure-volume-temperature data set indicate that a significant amount of magnesiowüstite is required to match PREM bulk modulus profile, thus making a pure perovskite lower mantle unlikely.

1. Introduction

Information required for interpretation of seismological models of the Earth includes P-V-T equation of state data under the wide range of P-T conditions prevailing in the mantle. A wealth of thermoelastic properties has thus been collected during the past few years on important mantle minerals, such as olivine and its high-pressure polymorphs, pyroxenes, garnets, ilmenite and stishovite. The study of the Earth's deep interior has made people focus on $(Mg,Fe)SiO_3$ perovskite and (Mg,Fe)O magnesiowüstite, considered to be the two main phases of the lower mantle. Bulk moduli (K_T) and pressure and temperature derivatives are being increasingly well constrained by synchrotron-based X-ray diffraction P-V-T studies [*Fei et al.*, 1992; *Fiquet et al.*, 1998; *Funamori et al.*, 1996; *Mao et al.*, 1991; *Wang et al.*, 1994]. Few studies, however, have been able to achieve P-V-T measurements on $MgSiO_3$ perovskite samples under the actual pressure and temperature conditions of the lower mantle. *Fiquet et al.* [1998] measured the unit-cell parameters of the silicate perovskite up to pressures of 57 GPa and temperatures in excess of 2500 K.

A new series of experiments recently allowed us to achieve X-ray diffraction measurements to 94 GPa at high temperature, which are reported here. These experiments give new constraints on the P-V-T equation of state of $MgSiO_3$ perovskite, as well as on the detailed high-pressure high-temperature structural behavior of this perosvkite. These results will be discussed to address the following points: (1) the stability field of $MgSiO_3$ perovskite, (2) the structure response to extreme pressure and temperature conditions, (3) the thermal equation of state of that compound and (4) the implications for the Earth's lower mantle composition.

2. Experimental

Angle-dispersive X-ray diffraction experiments were carried out at high pressure and temperature in a laser-heated diamond-anvil cell at the ID30 dedicated high-pressure beamline of the ESRF (Grenoble, France). A detailed description of the laser-heating and diamond-anvil cell experimental set-up can be found elsewhere [*Fiquet et al.*, 1996]. A doubly focused monochromatic X-ray beam was used at wavelengths set between 0.4 and 0.5 Å in association with imaging plates and the fast scan technique available on the high pressure beamline of the ESRF to collect data over a 2θ interval from 4 to 25° (see *Andrault et al.* [1997] or *Fiquet et al.* [1998] for details). Wavelength as well as sample-detector distance were calibrated against a Si standard and standards for absorption edges. X-rays were focused to a spot of about 10 x 15 µm FWHM on the sample and data collected at each temperature for 2 to 5 minutes.

$MgSiO_3$ perovskite samples were synthesized (1) from synthetic $MgSiO_3$ enstatite and (2) from synthetic $MgSiO_3$ glass, mixed with platinum powder and transformed at high pressure and high temperature into perovskite-type $MgSiO_3$. These starting materials were loaded cryogenically in argon, which was used as pressure transmitting medium, or compressed without any pressure transmitting medium for the experiments performed above 50 GPa. Samples were either heated with a stabilized TEM00 CO_2 laser (λ = 10.6 µm, model 57-1-28 W from Synrad) for experiments carried out in argon below 50 GPa or with a stabilized high-power multimode Nd:YAG laser (λ = 1.06 µm, model 118F/CW from Quantronix) for experiments carried out above 50 GPa. Re gaskets with holes 70-100 µm in

Table 1. Volume measurements of $MgSiO_3$ perovskite at various pressure and temperature conditions

T (K)	P (GPa)	V (Å^3)	T (K)	P (GPa)	V (Å^3)
298	46.88 (30)	140.827 (54)	*298*	75 06 (30)	132.728 (17)
298	50.94 (30)	139.810 (28)	*298*	75.62 (30)	132.788 (17)
298	53.63 (30)	139.269 (24)	*298*	40.03 (30)	143.442 (20)
298	53.46 (30)	139.307 (43)	*298*	42.17 (30)	142.588 (15)
298	85.70 (30)	130 097 (22)	*298*	39.44 (30)	143.328 (20)
298	90.17 (30)	129 303 (24)	*298*	40.66 (30)	143.255 (23)
298	90.57 (30)	129 292 (17)	*2897*	67.41 (45)	139.549 (26)
298	38.63 (30)	143.777 (19)	*2963*	67.23 (79)	139.783 (34)
298	45.38 (30)	141.332 (27)	*1179*	94.15 (51)	129.656 (14)
298	46.44 (30)	141 200 (25)	*1763*	46.87 (80)	144.414 (30)
298	80.57 (30)	131.651 (23)	*1889*	52.21 (46)	142.652 (18)
298	29.50 (30)	147.178 (15)	*2372*	54.14 (46)	142.176 (29)
298	31.57 (30)	146.567 (18)	*1995*	88.00 (46)	132.296 (21)
298	31.47 (30)	146.537 (12)	*1380*	91.82 (82)	130.768 (27)
298	85.32 (30)	130.266 (12)	*1681*	79.74 (87)	133.829 (11)
298	70.12 (30)	133 641 (08)	*1603*	81.81 (68)	133.160 (14)
298	71.50 (30)	133.598 (14)	*1918*	46.78 (80)	144.319 (26)
298	65.88 (30)	135.058 (19)	*2199*	46.98 (63)	145.408 (68)
298	67.94 (30)	134.801 (27)	*1845*	43.09 (112)	145.464 (48)

[1]Laboratoire de Sciences de la Terre, Ecole Normale Supérieure de Lyon, Lyon, France

[2]Now at Laboratoire de Minéralogie et Cristallographie, Université Pierre et Marie Curie (Paris VI), Case 115, Tour 16, 2ème étage, 4 Place Jussieu, 75252 Paris cedex 05 (e-mail: fiquet@lmcp jussieu.fr)

[3]Département des Géomatériaux, Institut de Physique du Globe de Paris, Paris, France

[4]Laboratory of Crystallography, ETH Zentrum, Zuerich, Switzerland

[5]ESRF, Grenoble, France

Copyright 2000 by the American Geophysical Union.

Paper number 1999GL008397.
0094-8276/00/1999GL008397$05.00

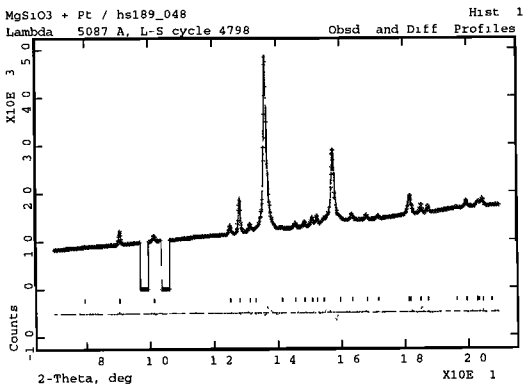


Figure 1. Integrated angle dispersive X-ray diffraction pattern collected at 79.7 GPa and 1681 K. Exposure time 5 minutes at wavelength λ = 0.5087 Å. Dashes, upper and lower solid lines represent experimental, calculated and difference spectra, respectively (see Table 2 for the details of refinement). Lower ticks: perovskite; upper ticks: platinum.

diameter were used. Temperatures were measured from the analysis of the sample thermal emission, collected every 5 seconds during the X-ray diffraction experiment with an optical set-up designed for this purpose [*Fiquet et al.*, 1996]. Because sample thickness was between 10 and 15 μm, we assume that the axial temperature gradient was negligible in such transparent samples. This assumption is supported by the experimental evidence of diffraction peak widths during laser-heating (0.05-0.08 degrees-2θ) which are comparable to ambient conditions Si-standard (0.02-0.05 degrees 2θ). Pressures were inferred from the equation of state (EoS) of platinum [*Jamieson et al.*, 1982], used as an internal pressure calibrant. Temperature fluctuations recorded during the experiments have also been taken into account through the platinum P-V-T equation of state and appear in the pressure uncertainties reported in Table 1.

2-D images were integrated after spatial distortion and background corrections using program Fit2d [*Hammersley*, 1996] and treated using GSAS package [*Larson and Von Dreele*, 1988]. Le Bail profile refinements were applied to the diffraction patterns, in order to obtain reliable high-pressure high-temperature cell parameters for $MgSiO_3$ perovskite as well as for the pressure calibrant. In these experiments, a total of 20 reflections were used to refine the cell parameters of $MgSiO_3$ perovskite. Rietveld structural refinements were achieved on selected patterns at extreme pressure and temperature conditions, yielding detailed structural information on this compound (see Figure 1 and Table 2). In this last step, up to 24 parameters were adjusted for the background, the cell parameters of $MgSiO_3$ perovskite, platinum, or argon as well as two peak profiles for each compound, and atomic positions for the perovskite sample.

P-V-T data set was then fitted to a Birch-Murnaghan equation of state modified to take into account temperature effect on bulk modulus. We used a numerical code based on the generalized least squares inversion scheme of *Tarantola and Valette* [1982] to invert from the whole data set the ambient molar volume V_0, the room-temperature bulk modulus K_0, its first pressure derivative K'_0 as well as the first temperature derivative $(\partial K/\partial T)_P$, and the thermal expansion coefficients assuming an empirical expression $[\alpha = \alpha_0 + \alpha_1 T + \alpha_2 T^{-1}]$. Alternatively, we used a Mie-Grüneisen equation of state to constrain the Grüneisen parameter γ and the q parameter (see *Jackson* [1998]).

Table 2. Refined unit-cell, atomic coordinates and selected interatomic distances (Å) and angles (in degrees) for $MgSiO_3$ perovskite at 79.7 GPa and 1681 K.

Atom	x	y	z
Mg	0.5182(14)	0.5817(12)	¼
Si	½	0	½
O(1)	0.1069(21)	0.4755(26)	¼
O(2)	0.1883(16)	0.1939(16)	0 5621(13)
Bond distances			
Si-O(1) x2	1 686(3)	Mg-O(1) x1	1.894(11)
Si-O(2) x2	1 702(7)	Mg-O(1) x1	1.919(12)
Si-O(2) x2	1.703(8)	Mg-O(2) x2	1.922(8)
		Mg-O(2) x2	2.066 (10)
		Mg-O(2) x2	2.275 (10)
		Mg-O(1) x1	2.663(11)
		Mg-O(1) x1	2.882 (12)
Mean <Si-O>	1.697	Mean <Mg-O>	2.188
Bond angles			
Si-O(1)-Si	146.3(6)	Si-O(2)-Si	142.2(5)

U_{iso} not refined and fixed to the values of *Ross and Hazen* [1990]. The final discrepancy indices [*Larson and Von Dreele*, 1988] are *Rwp*= 0.013, *Rp*= 0.007, $R(F^2)$= 0.070 and reduced $\chi 2$= 0.151. Space group: *Pbnm*, Z=4, *a*= 4.4449(4) Å, *b*= 4.6648 (4) Å, *c*= 6.4544 (4) Å, mixture composed of 86 wt% of $MgSiO_3$ perovskite and 14 wt% platinum.

3. Results and discussion

3.1. Stability field

Pressure-volume-temperature data are reported in Table 1. As shown in this table, diffraction patterns were recorded up to 94 GPa and almost 3000 K. In this pressure-temperature range, the patterns indicate that the *Pbnm* orthorhombic structure is stable. We do not observe any phase transition or dissociation to an assemblage of perovskite and oxides, i.e. MgO and SiO_2, as observed by *Meade et al.* [1995] or *Saxena et al.* [1996]. This dissociation has been indeed observed above 65 GPa in the latter studies, which is in contradiction with our observations for at least five of our runs where orthorhombic perovskite was observed at pressures varying from 67 to 88 GPa combined with temperatures close to or exceeding 2000 K (see Figure 1 for example). On the other hand, our results confirm experiments carried out by *Mao et al.* [1997] who reported $MgSiO_3$ perovskite was stable to at least 80 GPa and by *Serghiou et al.* [1998], where perovskite was formed from oxides at pressures exceeding 100 GPa, both in laser-heated diamond-anvil cells. Furthermore, thermodynamic calculations show an extended pressure and temperature stability field for $MgSiO_3$ perovskite, when the denser high-pressure post-$CaCl_2$ structured SiO_2 polymorph reported by *Dubrovinsky et al.* [1997] is not taken into account [*Matas et al.*, in preparation]. Note however that this new silica phase is controversial since recent X-ray

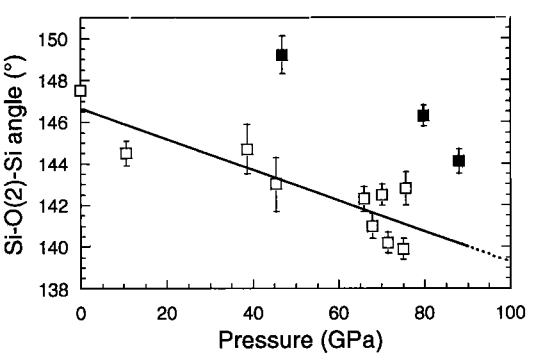


Figure 2. Measured tilt angle [Si-O(2)-Si] for $MgSiO_3$ perovskite as a function of pressure and temperature. The data points at room-pressure and 10 GPa are from Ross and Hazen [1990]. The increase of the orthorhombic distortion with increasing pressure, i.e. the decrease of the [Si-O-Si] angle, is obvious. The data collected at high-temperature (solid squares), on the other hand, show a decrease of this distortion.

diffraction experiments report the $CaCl_2$ structure of SiO_2 up to 120 GPa [*Andrault et al.*, 1998]. These results thus make the breakdown of perovskite to a denser assemblage of simple oxides very unlikely. The experimental observations of *Meade et al.* [1995] or *Saxena et al.* [1996] most likely originated in disequilibrium associated with large temperature gradients in the Nd-YAG laser-heating technique [e.g. *Yagi et al.*, 1997].

3.2. Structural evolution at high-pressure and high-temperature

The wide range of structural distortion away from the ideal cubic in perovskite-structured compounds had raised the possibility of pressure and/or temperature induced changes in the symmetry of $(Mg,Fe)SiO_3$ phases (see *Wang et al.* [1992]). Our new measurements demonstrate a wide P-T stability field for the Pbnm orthorhombic phase and a large compression anisotropy along *a*, *b*, *c* axes. The axial compressibilities calculated from least-squares fits of the compression data are 1.23×10^{-3} GPa^{-1}, 0.98×10^{-3} GPa^{-1} and 1.21×10^{-3} GPa^{-1} for *a*, *b* and *c* axes respectively. This is in good agreement with results reported from a single crystal study by *Ross and Hazen* [1990] and compatible with an increase of the orthorhombic distortion with increasing pressure. Rietveld refinements done on selected patterns also yield detailed structural information on $MgSiO_3$ perovskite at high pressure and high temperature (see Table 2 and Figure 2). We observe, for instance, a clear trend in the evolution of the Si-O(2)-Si angle with pressure and temperature, with a significant decrease of the Si-O(2)-Si angle (i.e. increase of the orthorhombic distortion) with increasing pressure (Figure 2). On the other hand, we notice a decrease of this orthorhombic distortion mainly accomodated by a Si-O(2)-Si angle increase with increasing temperature at high pressure. In no case, however, was this angle variation large enough to come close to a tetragonal or cubic structure (i.e., Si-O-Si angles of 180°). The fact that the most important part of the distortion lies inside the Si-O-Si angle is well described (e.g. *Sasaki et al.* [1983]) and directly translates into the anisotropy in axial compression described above. In the same manner, the decrease of the orthorhombic distortion with increasing temperature observed even at high pressure agrees very well with the previous reports of *Ross and Hazen* [1989] and *Parise et al.* [1990], and shows that the behavior of $MgSiO_3$ perovskite with temperature mirrors its behavior under compression. Still, our measurements show that $MgSiO_3$ perovskite remains highly distorted under high-pressure conditions even at high temperature. The structural refinement results reported in Table 2 indeed yield a tolerance factor t_{obs} of 0.912 (t_{obs}=1 for an ideal cubic perovskite). It thus seems most likely that the *Pbnm* orthorhombic $(Mg,Fe)SiO_3$ perovskite phase remains stable relative to perovskites of higher symmetry along plausible lower mantle geotherms. Refinements carried out above 50 GPa also show that the assumption that SiO_6 octahedra are essentially rigid is questionable. Although most of the distortion with pressure is tilting of the octahedra, the degree of distortion and compression within the octahedra also changes under pressure or temperature. At around 70 GPa for instance, octahedra undergo almost 15% compression. Volume compression is thus also partly controlled by the shrinkage of Si-O bond lengths, which might take place at rather high pressures when the Si-O-Si tilting and thus the MgO_{12} dodecahedron compression cannot be easily further increased.

3.3. Thermal equation of state

The room-temperature equation of state defined by the volume data recorded at room temperature after laser heating is in very good agreement with previous studies carried out under quasi-hydrostatic conditions, thus pointing out once again the efficiency of high-temperatures in releasing deviatoric stresses accumulated upon compression. The fit to a Birch-Murnaghan equation of state truncated to 3rd order yields a bulk modulus K_0 of 253(9) GPa, a pressure derivative K'_0= 3.9(2) and a room-pressure molar volume V_0= 162.27(1) Å^3. These results are in excellent agreement with the single crystal study of *Ross and Hazen* [1990] which yielded K_0= 254(13) GPa with K'_0 fixed to 4, as well as with our previous study in which K_0 was found to be 256(7) GPa [*Fiquet et al.*, 1998]. This bulk modulus is also compatible with previous measurements to 30 GPa by *Mao et al.* [1991] who reported 261 GPa (K'_0= 4).

Table 3. Parameters extracted from thermal equation of state for $MgSiO_3$ perovskite

Parameters	*A priori* parameters	(1)	(1)	(2)
V_0 (Å^3)	162.3 (fixed)	162.3	162 3	162.3
$K_{0,T}$(GPa)	261	259	259.5 (9)	267.6 (9)
$K'_{0,T}$	4	3.7	3 69 (4)	3.78 (3)
$(\partial K/\partial T)_P$ ($GPaK^{-1}$)	-0.02		-0.017 (2)	-0.021 (2)
α_0 (10^{-5} K^{-1})	2		2.18 (12)	1.54 (4)
α_1 (10^{-8} K^{-2})	0.8		0.11 (8)	0.92 (9)
Θ_D		1100 K (fixed) †		
γ_0		1.4 ‡		
q		1.4 (5)		

(1) optimized from data set presented in Table 1 and that of *Fiquet et al.* [1998], (2) optimized from data sets of *Wang et al.* [1994], *Funamori et al.* [1996] and *Saxena et al.* [1999]. 63 and 213 data points for data sets (1) and (2) respectively.

† Θ_D value from *Anderson* [1998]

‡ preferred γ_0 value from the range of values calculated at room conditions by *Jackson and Rigden* [1996]

Results of the inversion of the entire data set combined with that of *Fiquet et al.* [1998] are reported in Table 3. A *posteriori* errors on parameters were calculated from the resolution matrix assuming normally distributed errors and molar volume V_0 fixed to 162.3 Å^3. A fit to a combination of data sets by *Wang et al.* [1994], *Funamori et al.* [1996] and *Saxena et al.* [1999] is included for comparison. From our new data, we obtained a $(\partial K/\partial T)_P$ value of -0.017(2) $GPaK^{-1}$. Although this value is slightly smaller than previous measurements found in the literature, i.e. $(\partial K/\partial T)_P$= -0.020 $GPaK^{-1}$ [*Utsumi et al.*, 1995], -0.023(11) $GPaK^{-1}$ [*Wang et al.*, 1994], -0.027(5) $GPaK^{-1}$ [*Fiquet et al.*, 1998; *Saxena et al.*, 1999] and -0.028(17) $GPaK^{-1}$ [*Funamori et al.*, 1996], all these results almost agree within error bars. On the other hand, these results differ significantly from the extreme value of -0.063(5) $GPaK^{-1}$ reported by *Mao et al.* [1991].

The large pressure range explored in this study allows us to put strong constraints on the first pressure derivative of the incompressibility, which is lower than 4 (K'_0= 3.69, see table 3). Surprisingly, a combination of all data is not efficient in constraining higher order terms such as $(\partial^2K/\partial T^2)$, $(\partial^2K/\partial P\partial T)$ and the α_2 term in the thermal expansion expression. Another frequently used thermal equation of state is the Debye Mie-Grüneisen equation of state (see [*Fei et al.*, 1992; *Jackson*, 1998]). As illustrated in *Bina* [1995], the trade-off between the *q* parameter $(\partial \ln \gamma / \partial \ln V)_T$ and the Grüneisen parameter γ_0 is not well constrained. As shown in Table 3, we obtain a value of 1.4±0.5 for *q* when assuming a Grüneisen parameter γ_0 of 1.4, as obtained in the recent spectroscopic estimates of *Gillet et al.* [1996] and *Jackson and Rigden* [1996].

3.4. Geophysical implications

These new data on $MgSiO_3$ perovskite allow us to examine the effect of this material on constraining the composition of the lower mantle. With equation of state parameters listed Table 3, we calculate density and K_T for $MgSiO_3$ perovskite along a plausible lower mantle geotherm assuming a zero-depth foot temperature of 1830 K, which can be compared with density and K_T profiles calculated from PREM. The predicted density for a

pure (Mg,Fe)SiO_3 perovskite with 7% iron lower mantle is indistinguishable from PREM profiles. On the other hand, the K_T values are about 4-7 % higher than those predicted from the K_T profile of PREM, calculated after *Brown and Shankland* [1981]. About 10% (Mg,Fe)O is thus required to match the Earth's K_T profile under the hypothesis of a three-component lower mantle. Within the framework of a four components lower mantle [MgO, FeO, CaO and SiO_2], (Mg+Fe+Ca)/Si of 1.08(2) and Fe/(Fe+Mg)= 0.11(5) yield a density and bulk modulus that are consistent with those of PREM. In these calculations, the partitioning coefficient of iron between magnesiowüstite and perovskite was assumed to be constant and equal to 3 [e.g. *Martinez et al.*, 1997]. We assumed 8 vol% $CaSiO_3$ perovskite with thermoelastic parameters of *Wang et al.* [1996]. For magnesiowüstite, we used the P-V-T equation of state of *Fei et al.* [1992]. These results, although slightly different from those presented in *Fiquet et al.* [1998], make a pure perovskite lower mantle unlikely, in good agreement with conclusions drawn from previous experiments by *Wang et al.* [1994], *Funamori et al.* [1996], *Saxena et al.* [1999] or calculations by *Gillet et al.* [1996] or *Jackson and Rigden* [1996].

Still, a pure silicate perovskite lower mantle composition would also satisfy PREM density and bulk modulus profiles when the zero-depth foot temperature of the lower mantle adiabat is fixed to 2400 K instead of 1830 K. It must be also noted that no *in situ* experimental study has been for the moment able to clearly show the effect of iron substitution on the thermal equation of state of (Mg,Fe)SiO_3 perovskite. The shift in thermal expansivity with increasing iron content, however, seems to be rather small [*Anderson and Hama*, 1999]. Aluminium is also a very important component that has to be taken into account since the 4 or 5 mole percent of aluminium oxide (Al_2O_3) present for all proposed mantle compositions is believed to be incorporated into (Mg,Fe)SiO_3 perovskite [*Irifune et al.*, 1996]. Al_2O_3 has been shown to have a large influence onto the thermal equation of state [*Zhang and Weidner*, 1999]. In addition, other experimental studies on magnesiowüstite at lower mantle pressure and temperature conditions are needed for a better refinement of lower mantle compositional models.

Acknowledgments. We would like to thank the ECC (ESRF Extreme Conditions Consortium) for the loan of the multimode Nd-YAG infrared laser used in this study, as well as S. Bauchau for his help at the ID30 beamline. We thank J. Matas for the development of the inversion code and R.J. Hemley for his comments on the manuscript. Detailed and constructive reviews by C.R. Bina and J. Zhang are appreciated. This work has been possible under the auspices of INSU-CNRS Programme "Terre Profonde"

References

Anderson, O.L., Thermoelastic properties of $MgSiO_3$ perovskite using the Debye approach, *Amer Mineral, 83*, 23-25, 1998

Anderson, O.L., and J Hama, Shifts in thermal expansivity with Fe content for solid solutions of $MgSiO_3$-$FeSiO_3$ with the perovskite structure, *Amer Mineral, 84*, 221-225, 1999

Andrault, D., G Fiquet, F Guyot, and M Hanfland, Pressure-induced Landau-type transition in stishovite, *Science, 282*, 720-724, 1998.

Andrault, D., G Fiquet, M Kunz, F Visocekas, and D Hausermann, The orthorhombic structure of iron an *in situ* study at high-temperature and high-pressure, *Science, 278*, 831-834, 1997

Bina, C.R., Confidence limits for silicate perovskite equations of state, *Phys. Chem Minerals, 22*, 375-382, 1995.

Brown, J M, and T J Shankland, Thermodynamic parameters in the Earth as determined from seismic profiles, *Geophys J. R Astron Soc, 66*, 579-596, 1981

Dubrovinsky, L.S., S K. Saxena, P. Lazor, R Ahuja, O Eriksson, J M. Wills, and B Johansson, Experimental and theoretical identification of a new high-pressure phase of silica, *Nature, 388*, 362-365, 1997

Fei, Y, H. Mao, and J. Hu, P-V-T equation of state of magnesiowüstite ($Mg_{0.6}Fe_{0.4}$)O, *Phys Chem. Minerals, 18*, 416-422, 1992.

Fiquet, G., D Andrault, A Dewaele, T. Charpin, M Kunz, and D. Häusermann, P-V-T equation of state of $MgSiO_3$ perovskite, *Phys. Earth Planet. Int, 105*, 21-31, 1998

Fiquet, G, D Andrault, J.P. Itié, P. Gillet, and P Richet, X-ray diffraction of periclase in a laser-heated diamond anvil cell, *Phys Earth Planet. Int., 95*, 1-17, 1996.

Funamori, N., T. Yagi, W. Utsumi, T Kondo, T. Uchida, and M Funamori, Thermoelastic properties of $MgSiO_3$ perovskite determined by in situ X ray observations up to 30 GPa and 2000 K, *J Geophys Res-Solid Earth, 101* (B4), 8257-8269, 1996.

Gillet, P, F Guyot, and Y Wang, Microscopic anharmonicity and the equation of state of $MgSiO_3$-perovskite, *Geophys Res Lett., 23*, 3043-3046, 1996.

Hammersley, J, Fit2d, *ESRF publication*, 1996

Irifune, T, T. Koizumi, and J I. Ando, An experimental study of the garnet-perovskite transformation in the system $MgSiO_3$-$Mg_3Al_2Si_3O_{12}$, *Phys Earth Planet Interiors, 96* (2-3), 147-157, 1996.

Jackson, I., Elasticity, composition and temperature of the Earth's lower mantle: a reappraisal, *Geophys J Int, 134*, 291-311, 1998

Jackson, I, and S.M. Rigden, Analysis of P-V-T data Constraints on the thermoelastic properties of high-pressure minerals, *Phys Earth Planet Interiors, 96* (2-3), 85-112, 1996.

Jamieson, J C., J.N Fritz, and M.H. Manghnani, Pressure measurement at high temperature in X-ray diffraction studies gold as a primary standard, in Akimoto, S, Manghnani, M H (eds), *High Pressure Research in Geophysics*, Reidel, Boston, 1982

Larson, A C., and R B Von Dreele, GSAS manual, report LAUR 86-748, Los Alamos National Laboratory, 1988.

Mao, H.K., R J Hemley, Y Fei, J F. Shu, L C Chen, A.P. Jephcoat, Y Wu, and W.A Bassett, Effect of pressure, temperature and composition on lattice parameters and density of (Mg,Fe)SiO_3-perovskite to 30 GPa, *J Geophys Res., 96*, 8069-8079, 1991

Mao, H K, G Shen and R.J Hemley, Multivariable dependence of Fe-Mg partitioning in the lower mantle, *Science, 278*, 2098-2100, 1997

Martinez, I, Y Wang, F Guyot, R C Liebermann and J C. Doukhan, Microstructures and iron partitioning in (Mg,Fe)SiO_3 perovskite-(Mg,Fe) magnesiowüstite assemblages: an analytical transmission electron microscopy study, *J Geophys Res, 102*, B3, 5265-5280, 1997.

Meade, C., H.K Mao, and J. Hu, High-temperature phase transition and dissociation of (Mg,Fe)SiO_3 perovskite at lower mantle pressures, *Science, 268*, 238, 1995.

Parise, J.B., Y. Wang, A. Yeganeh-Haeri, D E Cox, and Y. Fei, Crystal structure and thermal expansion of (Mg,Fe)SiO_3 perovskite, *Geophys. Res. Lett., 17* (12), 2089-2092, 1990.

Ross, N L, and R M. Hazen, Single crystal X-Ray diffraction study of $MgSiO_3$ perovskite from 77 to 400 K, *Phys Chem Miner* (16), 415-420, 1989.

Ross, N.L, and R.M Hazen, High-pressure crystal chemistry of $MgSiO_3$ perovskite, *Phys Chem Miner.* (17), 4228-4237, 1990.

Sasaki, S, C T. Prewitt, and R.C Liebermann, The crystal structure of $CaGeO_3$ perovskite and the crystal chemistry of the $GdFeO_3$-type perovskites, *Amer. Mineral, 68*, 1189-1198, 1983

Saxena, S K, L S Dubrovinsky, P Lazor, Y Cerenius, P Haggkvist, M. Hanfland, and J. Hu, Stability of perovskite ($MgSiO_3$) in the Earth's mantle, *Science, 274*, 1357-1359, 1996

Saxena, S K., L S Dubrovinsky, F Tutti, and T LeBihan, Equation of state of $MgSiO_3$ with the perovskite structure based on experimental measurements, *Amer. Mineral, 84*, 226-232, 1999.

Serghiou, G, A Zerr, and R. Boehler, (Mg,Fe)SiO_3 perovskite stability under lower mantle conditions, *Science, 280*, 2093-2095, 1998

Tarantola, A and B Valette, Generalized nonlinear inverse problems solved using the least squares criterion, *Rev Geophys., 20*, 219-232, 1982.

Utsumi, W, N Funamori, T. Yagi, E Ito, T Kikegawa, and O Shimomura, Thermal expansivity of $MgSiO_3$ perovskite under high pressures up to 20 GPa, *Geophys Res Lett, 22* (9), 1005-1008, 1995

Wang, Y., F Guyot, and R.C. Liebermann, Electron microscopy of (Mg, Fe)SiO_3 perovskite: evidence for structural phase transitions and implications for the lower mantle, *J Geophys Res, 97* (B9), 12,327-12,347, 1992.

Wang, Y.B, D J Weidner, and F. Guyot, Thermal equation of state of $CaSiO_3$ perovskite, *J Geophys Res-Solid Earth, 101* (B1), 661-672, 1996

Wang, Y B, D J Weidner, R C Liebermann, and Y.S Zhao, P-V-T Equation of State of (Mg,Fe)SiO_3 Perovskite - Constraints on Composition of the Lower Mantle, *Phys Earth Planet Interiors, 83* (1), 13-40, 1994

Yagi, T., B. O'Neill, T Kondo, N. Miyajima, and K Fujino, Post-garnet high-pressure transition effect of heterogeneous laser heating and introduction of some new techniques, *Eur. J Mineral, 9*, 301-310, 1997

Zhang, J, and D J Weidner, Thermal equation of state of aluminum-enriched silicate perovskite, *Science, 284*, 782-784, 1999.

G. Fiquet and A. Dewaele, Laboratoire de Sciences de la Terre, ENS Lyon, 46 Allée d'Italie, 69364 Lyon cedex 07, France.

D. Andrault, Département des Géomatériaux, IPG Paris, 4 Place Jussieu, 75252 Paris cedex 05, France.

M. Kunz, Laboratory for Crystallography, ETH Zentrum, Sonneggstr. 5, CH-8092, Zuerich, Switzerland.

T. Le Bihan, ID30 beamline, ESRF, BP220, 38043 Grenoble cedex, France

(Received July 7, 1999; revised October 25, 1999;
accepted November 3, 1999.)